



Original article

Synthesis and biological evaluation of novel pyranochalcone derivatives as a new class of microtubule stabilizing agents



Dong Cao^{a,1}, Xiaolei Han^{a,1}, Guangcheng Wang^a, Zhuang Yang^b, Fei Peng^a, Liang Ma^a, Ronghong Zhang^a, Haoyu Ye^a, Minghai Tang^a, Wenshuang Wu^a, Kai Lei^a, Jiaolin Wen^a, Jinying Chen^a, Jingxiang Qiu^a, Xiaolin Liang^a, Yan Ran^a, Yun Sang^a, Mingli Xiang^a, Aihua Peng^a, Lijuan Chen^{a,*}

^a State Key Laboratory of Biotherapy, West China Hospital, West China Medical School, Sichuan University, Keyuan Road 4, Gaopeng Street, Chengdu 610041, China

^b Chemistry College, Sichuan University, Chengdu, Sichuan 610064, China

ARTICLE INFO

Article history:

Received 18 October 2012

Received in revised form

2 January 2013

Accepted 7 January 2013

Available online 16 January 2013

Keywords:

Pyranochalcone

Tubulin

Anticancer activity

Microtubule stabilizing agents

ABSTRACT

Twenty-five novel pyranochalcone derivatives were synthesized and evaluated for their *in vitro* and *in vivo* antiproliferative activities. Among them, compound **10i** exhibited superior potent activity against 21 tumor cell lines including multidrug resistant phenotype with the IC₅₀ values ranged from 0.09 to 1.30 μM. In addition, **10i** significantly induced cell cycle arrest in G2/M phase, promoted tubulin polymerization into microtubules and caused microtubule stabilization. Further studies confirmed that **10i** significantly suppressed the growth of tumor volume in HepG2 xenograft tumor model. Our study demonstrated that **10i** could have beneficial antitumor activity as a novel microtubule stabilizing agent.

© 2013 Elsevier Masson SAS. All rights reserved.

1. Introduction

Tubulin which plays a crucial role in cell growth involved in the formation of the mitotic spindle [1,2] has been recognized as an attractive molecular target for anticancer agents recently [3]. Drugs attack microtubules by interfering with the dynamics of tubulin polymerization or dissociation, resulting in the mitotic arrest. Two major classes of anticancer agents exert their effectiveness involved in this mechanism [4], defined as microtubule destabilizing (*Vinca* alkaloids [5], Colchicine and Combretastatin [6,7]) and microtubule stabilizing agents (Taxol, Epothilone and Discodermolide).

Taxol (Paclitaxel), generally regarded as the first microtubule stabilizing agent [8,9], is one of the strongest chemotherapeutic agents currently used in clinic [10,11]. Three non-taxoid compounds have also been shown to stabilize microtubules: Epothilone A, Epothilone B [12] and Discodermolide [13]. These compounds share with Taxol the ability to promote tubulin polymerization into microtubules and block microtubule dynamics, resulting in abnormal

mitosis and apoptosis. However, these compounds have some limitations such as the drug resistance, high toxicity, difficulty of synthesis and complex isolation procedure. Recently, several small synthetic molecules that stimulate tubulin polymerization and induce microtubule stabilization have been reported as potential microtubule stabilizing agents (Compounds **1**, **2**, **3** in Fig. 1) [14–16]. The success of previous research encourages scientists to search for simple small molecules for microtubule stabilizing agents.

Millepachine, a natural pyranochalcone, was for the first time isolated from *Millettia pachycarpa* in our lab [17]. It exhibited a potent cytotoxic activity and induced apoptosis effects in several human cancer cell lines with an IC₅₀ values ranging from 1.51 to 4.0 μM [18]. Similar to other reported chalcones [19,20], the cytotoxic activity of millepachine is associated with tubulin [17,18]. The easily modification and structural similarity to Combretastatin A4 (CA4) of millepachine hint that millepachine might be a potential lead compound for anti-tumor drug via targeting tubulin and encourage us to establish more advanced structure–activity relationships (SAR) around millepachine.

It is well known that CA4 has three important pharmacophore components: two hydrophobic rings (rings A and B), a linking bridge between the two rings (Fig. 1). Similarly to the structure of CA4, millepachine has two aromatic rings and an unsaturated chain. Hence, we assumed that it is feasible to introduce a 3'-hydroxyl group

* Corresponding author. Tel.: +86 28 85164063; fax: +86 28 85164060.

E-mail address: lijuan17@hotmail.com (L. Chen).

¹ These authors contributed equally and should be considered as co-first authors.

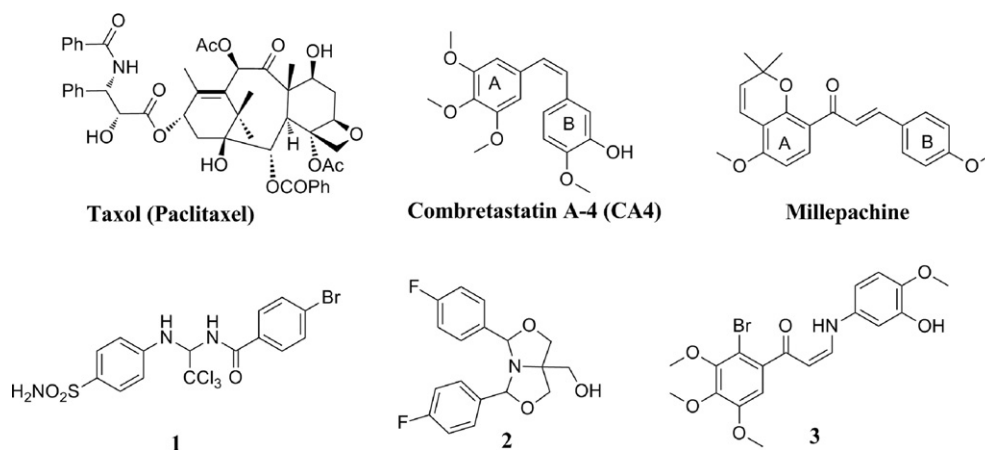


Fig. 1. Some tubulin interacting agents and lead structures.

on B ring and further modified on hydroxyl group of millepachine to obtain diverse derivatives. Herein, a series of millepachine-based pyranochalcones were synthesized and evaluated for their cytotoxicity in several human tumor cell lines including multidrug resistant phenotype. The effects on tubulin polymerization and the tumor cell cycle distribution of selected compounds were investigated to determine their exact mechanism. The most promising compound was further tested for anti-tumor activity and toxicity *in vivo*.

2. Results and discussion

2.1. Chemistry

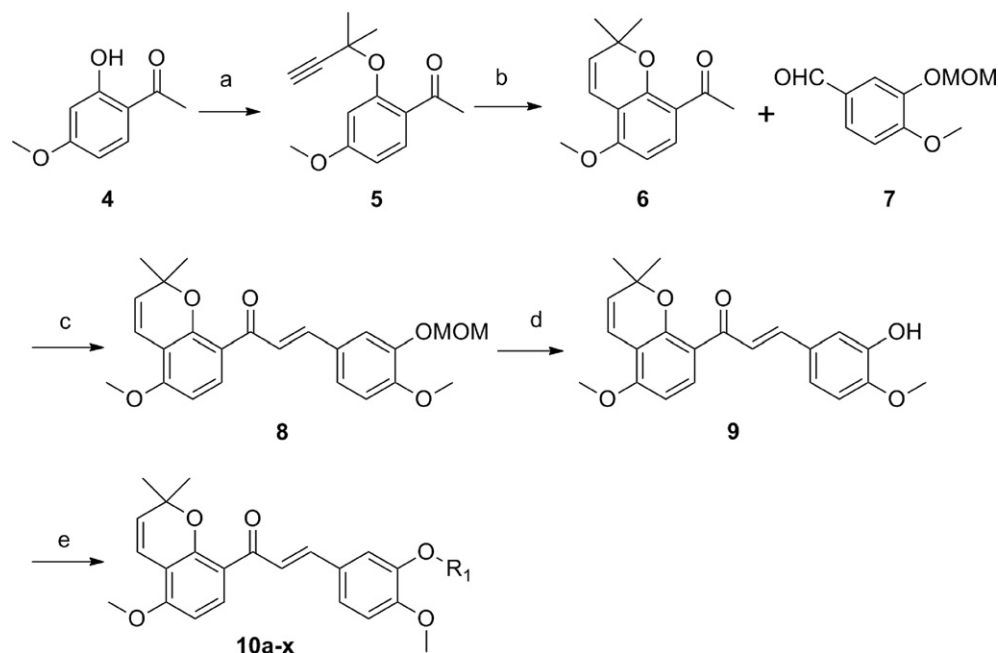
Although several synthetic approaches to pyranochalcones have been established [21–23], we reported an efficient and simple methodology for preparing naturally occurring pyranochalcones in previous work [24,25]. The Claisen–Schmidt condensation was used as a key procedure to synthesize the chalcone analogs, which proved to be satisfactory for the formation of *E* isomer [26,27] (Scheme 1).

The key intermediate **6** was prepared by condensation of paeonol **4** and 3-chloro-3-methyl-1-butyne, and followed cyclization upon heating in pyridine at 120 °C overnight. Subsequently, the chalcone analog **8** was obtained by Claisen–Schmidt condensation of **6** and aldehyde **7**. Although the synthetic procedure was suitable for a series of appropriate aldehydes, it had a low yielding or even unsuccessfully accomplished for the hydroxyl-substituent aldehydes because of the special chemical environment. To solve the problem, the hydroxyl-substituent benzaldehydes were initially protected by methoxy-methylene chloride (MOM-Cl), which was stable under the base-promoted condition. Compound **9** was readily obtained by the deprotection with dilute acid treatment, for the further generation of **10a–x**.

2.2. Biological activities

2.2.1. Biological activities *in vitro* cell growth inhibitory activity

The synthesized derivatives **9**, **10a–10x** were evaluated for antiproliferative activities *in vitro* by MTT assay against HepG2 cells



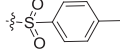
Scheme 1. Reagents and conditions: (a) 3-chloro-3-methylbut-1-yne, $\text{CuCl}_2 \cdot 2\text{H}_2\text{O}$, DBU, CH_3CN , 0 °C, 5 h; (b) Pyridine, 120 °C, 12 h; (c) NaOH (50% w/v aqueous solution), CH_3OH , rt, 12 h; (d) HCl/EA, rt, 2 h; (e) Method A for **10a–d**: K_2CO_3 , RCl , CH_3CN , reflux, 6 h; method B for **10e–h**: NaH, DMF, RCl , 12 h; method C for **10i–k**: $(\text{RCO})_2\text{O}$, pyridine, rt, 6 h; method D for **10l–n**: RCOCl , CH_2Cl_2 , rt, 6 h; method E for **10o–x**: RCOOH , EDCI, DMAP, CH_2Cl_2 , rt, 12 h.

Table 1
In vitro cytotoxicity of **9**, **10a–x**.

Comps	R	IC ₅₀ (μM)			
		HepG2	A375	K562	LO2
Millepachine	NA ^d	1.51	3.58	4.56	>20.0
9	H	0.45	0.80	0.63	>10.0
10a		>10.0	>10.0	>10.0	>10.0
10b		>10.0	>10.0	>10.0	>10.0
10c		>10.0	>10.0	>10.0	>20.0
10d		>10.0	9.60	8.75	>10.0
10e		>10.0	8.20	8.35	>10.0
10f		>10.0	3.81	3.05	9.50
10g		4.40	3.00	2.08	9.15
10h		5.55	4.10	2.92	8.60
10i		0.09	0.24	0.16	>10.0
10j		0.10	0.22	0.24	>10.0
10k		0.25	0.31	0.57	>10.0
10l		0.16	0.39	0.30	>10.0
10m		0.12	0.45	0.40	>10.0
10n		0.22	0.38	0.41	>10.0
10o		0.87	0.80	0.79	>10.0
10p		0.68	0.42	1.11	8.40
10q		0.57	0.48	0.29	>10.0
10r		0.60	0.70	0.43	>10.0
10s		0.43	2.63	0.38	18.0
10t		0.70	9.20	0.47	>10.0
10u		0.37	0.68	0.45	>10.0

(continued on next page)

Table 1 (continued)

Compds	R	IC ₅₀ (μM)			
		HepG2	A375	K562	LO2
10v		9.18	>10.0	9.24	>10.0
10w		>10.0	>10.0	>10.0	>10.0
10x		3.60	2.40	7.85	>10.0

^a NA, not applicable.

(human hepatocellular carcinoma), A375 cells (human melanoma), K562 cells (human leukemia) and LO2 cells (normal liver cell line) (Table 1). Generally, the antiproliferative activity of the most potent compounds was visibly greater against human liver HepG2 tumor cell lines as compared with the other cell lines.

The products by esterification were distinctly more potent than ether derivatives. The aliphatic products **10i–10n** displayed potent antiproliferative activities against tumor cell lines, particularly **10i** which showed the strongest activity against HepG2 cells and K562 cells (IC₅₀ 0.09 μM and 0.16 μM), and **10j**, the most active molecule against A375 cells (IC₅₀ 0.22 μM). However, the activities of products **10o–10t** which contained benzene ring in the substitutional group were sharply decreased. The ether derivatives **10a–10h** were the least active compounds in the series, with IC₅₀ values over 10 μM against almost all cell lines.

Then we tested the activity of the two compounds, **10i** and **10j**, against various human tumor cell lines, with Taxol and Colchicine as the positive controls. The tumor cells we evaluated included cancer cell lines coming from colon, lung, liver, breast, ovarian and prostate (Table 2). Similar to Taxol and Colchicine, the two compounds showed potent inhibitory activity with IC₅₀ values ranged from 0.1 to 0.5 μM against almost all cell lines except SPC-A1 and H460 lung cancer cell lines. It is worth notice that the IC₅₀ values of **10i** and **10j** (0.31 μM and 0.30 μM) showed around 3–5-fold increase than those of Taxol (1.05 μM) and Colchicine (1.72 μM) against C26 cells (murine colon adenocarcinoma). In general, the wide range of cell killing across multiple tumor types may suggest that this kind of compounds induce tumor cell killing by inhibiting an intrinsically important process of tumor cell division.

Table 2
Activity of selected compound against various human tumor cell lines.

Cell lines		IC ₅₀ of compds (μM)			
		10i	10j	Taxol	Colchicine
Colon	C26	0.31	0.30	1.05	1.72
	HCT-15	0.10	0.10	0.12	0.08
	HT29	0.20	0.19	0.45	0.02
Lung	NCI-H358	0.15	0.09	0.01	0.02
	SPC-A1	22.3	18.1	5.3	80
	H460	4.05	5.45	24	27
Liver	HepG2	0.09	0.10	0.19	0.21
	BEL-7402	0.40	>2.0	>2.0	1.31
	SK-HEP-1	0.32	0.60	0.24	0.17
Breast	MCF-7	0.19	0.25	0.66	0.29
	SK-OV-3	0.35	0.27	0.10	0.12
Ovarian	ES-2	0.10	0.10	0.10	0.09
	A2780S	0.22	0.33	0.02	0.02
Prostate	PC-3	0.09	0.12	0.14	0.04
	DU145	0.19	0.21	0.03	0.30
Drug resistant	MCF-7/ADR ^a	0.16	0.17	6.90	3.12
	HCT-8/T	1.69	2.30	13.3	11.8
	A2780/T	1.33	5.92	8.25	>20.0

Although many anticancer drugs in clinical use are effective, their potentials are limited by the development of drug resistance [28]. Thus, the antiproliferative effects of **10i** and **10j** were evaluated in MCF-7/ADR (multidrug-resistant human breast cancer cells), HCT-8/T (Taxol-resistant colon cancer cells), A2780/T (Taxol-resistant human ovarian cancer cells), compared with the tubulin interacting agents: Taxol and Colchicines (Table 2). These cell lines have been reported to express high levels of P-glycoprotein and were resistant to Taxol and Colchicine [28]. Compounds **10i** and **10j** were found to be sensitive both in sensitive and resistant cancer cells with similar IC₅₀ values ranged from 0.16 to 1.30 μM. For example, the IC₅₀ values of compound **10i** were respective 0.19 μM and 0.16 μM in MCF-7 and MCF-7/MDR, 0.22 μM and 1.33 μM in A2780 and A2780/T in contrast to Taxol, which was very sensitive to parental cell lines, was less active in the MCF-7/MDR cell line, with a shift in IC₅₀ values from 0.66 to 6.9 μM; and the Pgp-1 overexpressing cell line A2780/T, shifting its IC₅₀ values from 0.02 to 8.25 μM, showing 400-fold decrease in activity. The same results were obtained in Colchicine. These results show that the activities of **10i** and **10j** are not affected by Pgp-1 overexpressing, suggesting that **10i** and **10j** might be useful in the treatment of drug refractory tumors, in particular those with resistance to other antitubulin drugs.

2.2.2. Analysis of immunofluorescence staining

The biological activity of chalcones has been reported to be bound up with tubulin [19]. To investigate whether the antiproliferative activities of **10i** and **10j** were derived from an interaction with tubulin, we examined the effect on the cellular microtubule network treated with the selected compounds for 24 h and stained for DNA (blue) and α-tubulin (green). As shown in Fig. 2, in contrast with the microtubule network in HepG2 cells absence of drug exhibited normal arrangement and organization, after exposure the cells to 1 μM **10i** or **10j** for 24 h, the microtubule polymerization and spindle formation showed distinct abnormal. HepG2 cells became arrested in mitosis and the mitotic cells had abnormal mitotic spindles. The mitotic cells acquired multiple tubulin bundles (multipolar) without chromosomes aligned at the metaphase plate with more dispersion of the chromosomes. From the results obtained so far, it seems that tubulin might be an effective target for **10i** and **10j** (Fig. 2).

2.2.3. Analysis of cell cycle

Due to the anti-mitotic drugs induced cell cycle arrest at G2/M phase in various cancer cell lines and lead to an increment of the relative peak in the DNA histogram [29], the effects of compounds **10i**, **10j** at different concentration on cell cycle progression were examined in HepG2 cells. After treated 24 h, both **10i** and **10j** caused a remarkable G2/M arrest pattern in a concentration-dependent manner. When cells were treated with selected compound, an accumulation of tumor cells occurred the G2/M phase of the cell cycle, the G2/M peak raised from 17.07% (Control) to 67.76%

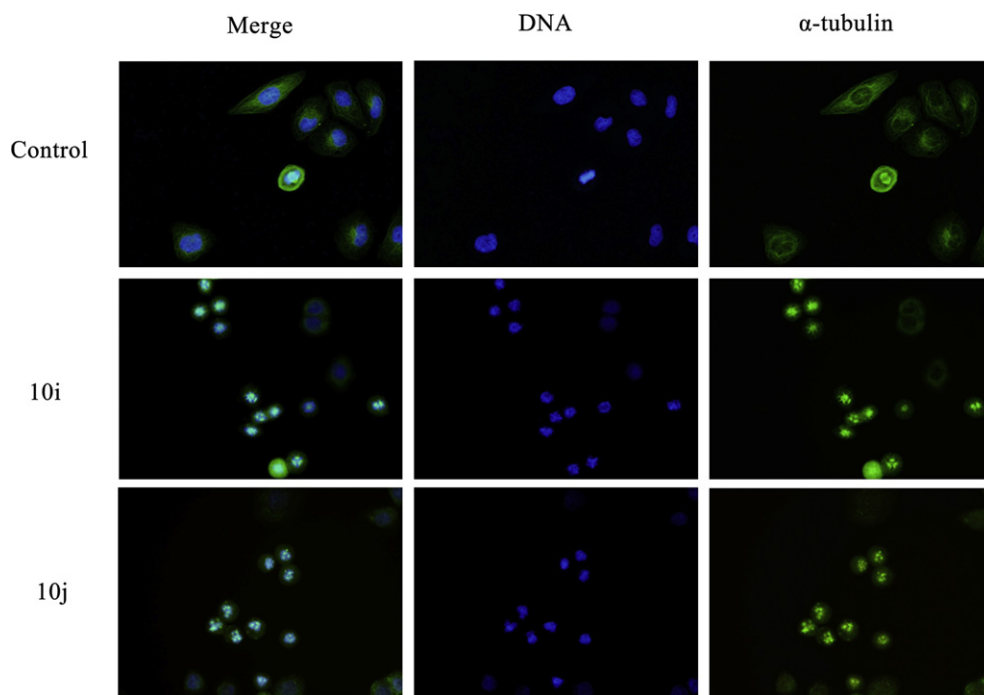


Fig. 2. Effects of **10i** and **10j** on the microtubule network of HepG2 cancer cells. Untreated (Control) and cells treated with **10i**, **10j** at concentration of 1.0 μM for 24 h, were fixed and stained with anti- α -tubulin-FITC specific antibodies followed by propidium iodide. Microtubules and unassembled tubulin are shown in green, and DNA, stained with propidium iodide is shown in blue. (For interpretation of the references to color in this figure legend, the reader is referred to the web version of this article.)

(**10i**), 53.47% (**10j**) at a concentration of 0.2 μM , and 76.02% (**10i**), 69.18% (**10j**) at a concentration of 1 μM , respectively. These trends were in accordance with the anti-mitotic drugs, further indicating that tubulin probably be an effective target for **10i** and **10j** (Fig. 3).

2.2.4. Tubulin polymerization assay

Since the structural similarity, we selected **10i** to further verify whether the activity of **10i** was related to the direct interaction with microtubules, the effects on the assembly of purified tubulin were evaluated by measuring an increase in absorbance at 340 nm at 37 °C [30]. In this experiment, Taxol, a microtubule stabilizer to enhance the rate of tubulin polymerization, was assessed as a positive control. Similar to Taxol, we found that **10i** did not depolymerize tubulin but stabilized tubulin polymerization, which was different from previous reports about chalcones [19,20]. As shown in Fig. 4, **10i** significantly and concentration-dependently stabilized tubulin polymerization. Treatment at respective 5, 10 and 20 μM of **10i** induced 10.0%, 16.3% and 32.0% increases of tubulin polymerization. At the same concentration, 5 μM and 20 μM of **10i** treatment showed stronger ability to promote the assembly of tubulin than Taxol (6.3% and 23.8%). This trend for accelerating tubulin polymerization was in good correlation with their cytotoxic activity, further ensuring that **10i** represents one novel microtubule stabilizing agent.

2.2.5. Western blot analysis

Given that tubulin binding molecules attack microtubules by interfering with the dynamics of tubulin polymerization or dissociation, we next studied the alterations in expression of tubulin that regulated cell division. Comparing to the control group, **10i** was characterized by increasing the level of polymerization-tubulin while decreasing the level of dissociation-tubulin. The experimental results further confirm that **10i** promoted tubulin polymerization into microtubules and induced microtubule stabilization (Fig. 5).

2.2.6. In vivo anticancer activity

The *in vivo* efficacy of **10i** was studied in s.c. xenograft models using human liver HepG2 tumor cell lines. HepG2 cells (5×10^6) were inoculated in each flank of null mice. Once tumor volume reached a size of around 100 mm^3 , **10i** was administered at doses of 2.5, 5, 10 mg/kg every two days. As the positive control, Taxol was injected at 5 mg/kg every four days. As shown in Fig. 6 and Table 3, during 20 days therapeutic treatment, **10i** was administered at 2.5, 5, 10 mg/kg dose-dependently inhibited tumor growth on day 20 (T/C = 34.9%, 32.4% and 33.9%, respectively), while the T/C of Taxol at 5 mg/kg was 32.4%. Tumor growth inhibition was extremely distinct in mice treated with **10i** at 10 mg/kg/2days. Compared with positive control, treatment with **10i** at 10 mg/kg resulted in the inhibitory rate of 69.7% and compared with mice treated by Taxol with an inhibitory rate of 59.1%.

During the therapeutic treatment, no distinct changes in gross measures were observed, including weight loss, feeding, and behavior. It was demonstrated that **10i** did not cause serious toxicity in mice at doses that associated with remarkable anti-tumor effects. All these results showed that **10i** could inhibit tumor growth significantly and seemed more safety than Taxol when possessing a similar tumor suppression. The exact mechanism still needs further research.

3. Conclusion

In our research, we described the synthesis of a series of mil-lepachine derivatives, which induced apoptotic death of a wide variety of tumor cell lines in the double-digit nanomolar range by attacking microtubules. Compound **10i** exerted the most potent activity in several human tumor cell lines including multidrug resistant human tumor cell lines. A flow cytometric study showed that compound **10i** significantly induced cell cycle arrest in G2/M phase at 0.2 μM . Furthermore, *in vitro* immunofluorescence staining and tubulin polymerization assay displayed that **10i**, similar to

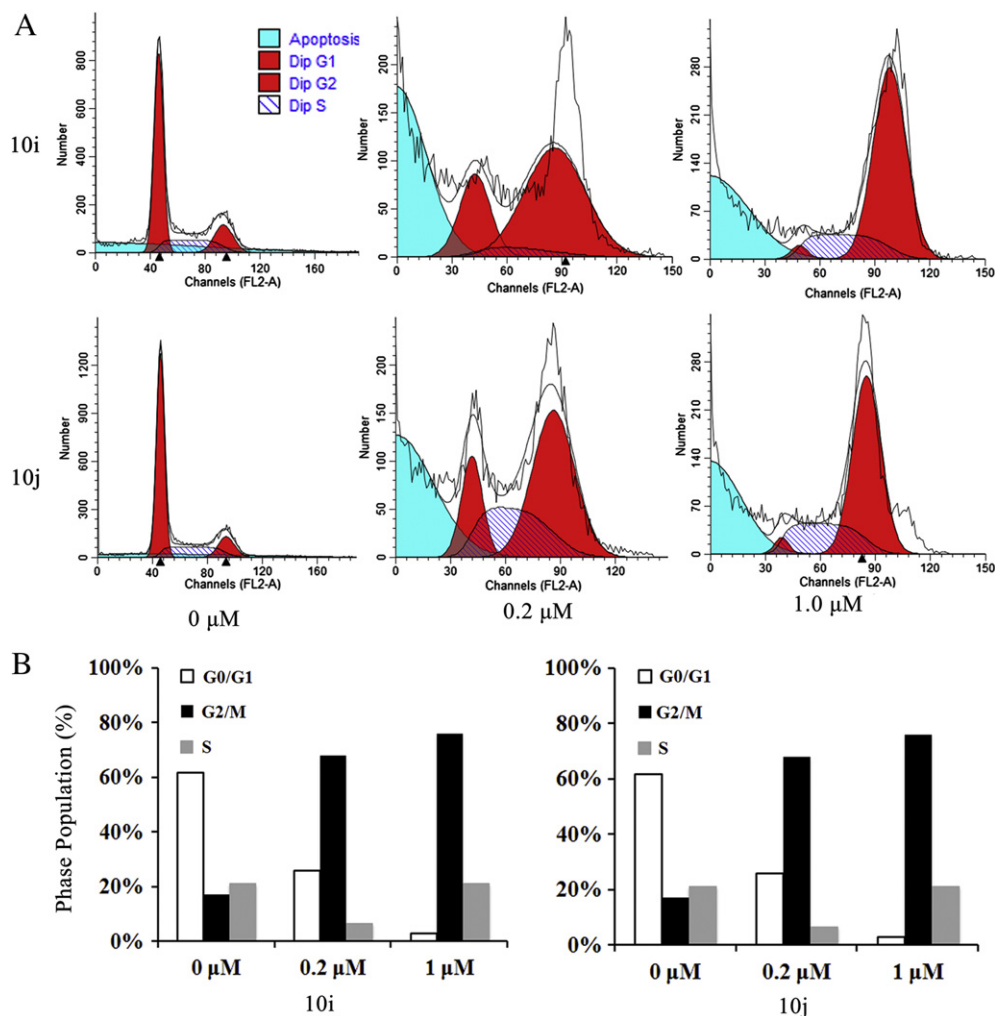


Fig. 3. **10i** and **10j** affected the cell cycle distribution in HepG2 cancer cells. Untreated (Control) and cells treated with **10i** and **10j** at 0.2 μM , 1.0 μM concentration for 24 h.

Taxol, promoted tubulin polymerization into microtubules and caused microtubule stabilization, which suggesting that compound **10i** is a microtubule stabilizer via enhancing the rate of tubulin polymerization. This result was also evidenced by western blot

analysis of the level of polymerization-tubulin. Comparing to the control group, **10i**, characterized by increasing the level of polymerization-tubulin while decreasing the level of dissociation-tubulin, was suggested to promote tubulin polymerization into microtubules and induced microtubules stabilization. Then *in vivo* study, compound **10i** exhibited potent inhibitory activity in human HepG2 xenograft tumor models. This study demonstrated that **10i** was supposed to be a new microtubule stabilizing agent and provided a new molecular scaffold for the further development of anti-

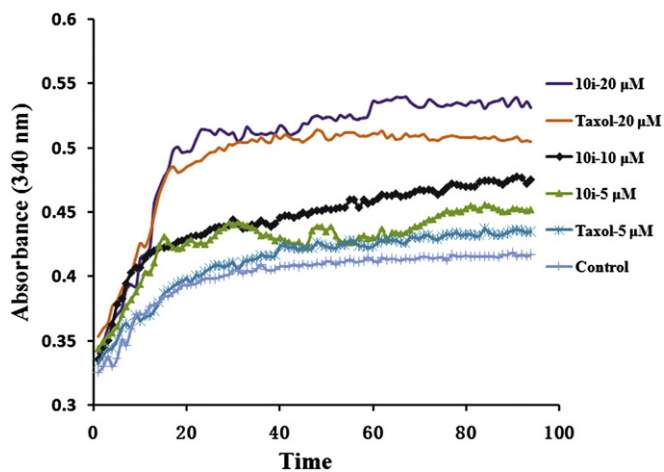


Fig. 4. Effect of **10i** on tubulin polymerization. Tubulin had been pre-incubated for 5 min with **10i** at 5 μM , 10 μM and 20 μM , Taxol at 5 μM and 20 μM or vehicle DMSO at room temperature before GTP was added to start the tubulin polymerization reactions. The reaction was monitored at OD340 nm at 37 $^{\circ}\text{C}$. Taxol was included as positive control.

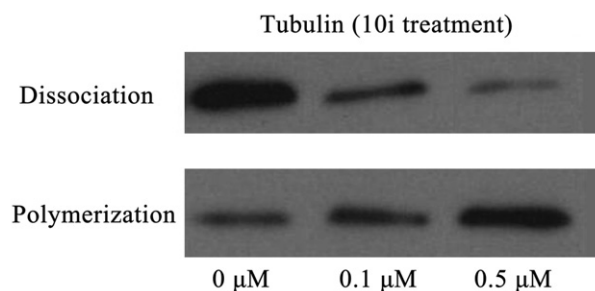


Fig. 5. **10i** affected the proportion of assembled tubulin. HepG2 cancer cells were treated with compound **10i** at 0.1 μM or 0.5 μM concentration. Comparing to the control, the proportion of assembled tubulin was increased, and the level of unassembled tubulin was decreased.

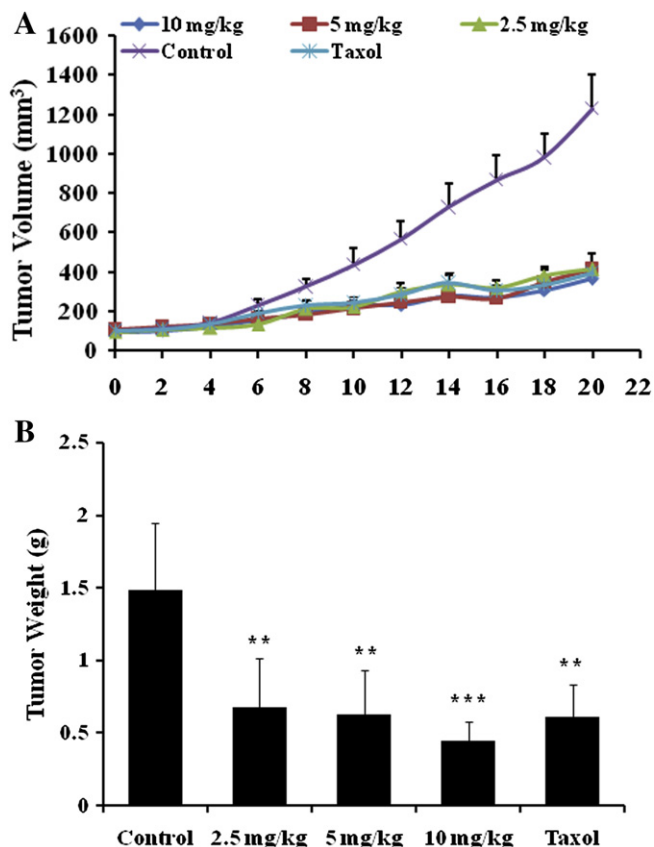


Fig. 6. **10i** inhibits the growth of HepG2 xenograft tumor. (A) The curves of inhibition of tumors. The three test groups were administered with 2.5, 5, 10 mg/kg of **10i** every two days. The positive group received Taxol at a dosage of 5 mg/kg every four days, and the control group received injection of physiological saline alone. Each group contained 6 mice. (B) The bar charts of tumor weight and the inhibitory rate of **10i**. *, $P < 0.05$, **, $P < 0.01$, and ***, $P < 0.001$, significantly different compared with control by *t* test.

tumor agents. In the future research we will be exploring for a clear structure activity relationship of this type of compound and discovering more potent anti-tumor agents.

4. Experimental

4.1. Chemistry

Chemistry reagents of analytical grade were purchased from Changzheng Chemical Factory, Chengdu, Sichuan, PR China. TLC was performed on 0.20 mm Silica Gel 60 F₂₅₄ plates (Qingdao Ocean Chemical Factory, Shandong, China). Proton (¹H) and carbon (¹³C) NMR spectra were recorded at 400 MHz and 100 MHz, respectively, on a Varian spectrometer (Varian, Palo Alto, CA) model Gemini 400 and reported in parts per million. Mass spectra (MS) were

Table 3
Summary of tumor growth inhibition.

Tumor	Compds	Dose (mg/kg/injection)	Inhibition rate (100%)	T/C value ^a (100%)
HepG2	10i	2.5	54.3	34.9
	10i	5	57.6	32.4
	10i	10	69.7	33.9
	Taxol	5	59.1	32.4

^a T/C value < 42% is considered as significant antitumor activity by the Drug Evaluation Branch of the Division of Cancer Treatment (NCI).

measured by Q-TOF Premier mass spectrometer (Micromass, Manchester, UK).

4.1.1. General preparation of **10a–d** (method A)

To a solution of compound **9** (0.365 g, 1 mmol) in anhydrous CH₃CN (10 mL) was added anhydrous K₂CO₃ (0.345 g, 2.5 mmol, 2.5 equiv). After stirred over 15 min at room temperature, requisite halogenated compound (2 mmol, 2 equiv) was added into the slurry. The reaction mixture was stirred at room temperature for 6 h. The reaction mixture was filtered, diluted with EtOAc and subsequently washed with water, then brine. The organic layer was dried over sodium sulfate and concentrated in vacuo. The resulting residue was purified by flash chromatography using petroleum ether/ethyl acetate (4:1) as eluent to yield light yellow solids.

4.1.1.1. (E)-1-(5-Methoxy-2,2-dimethyl-2H-chromen-8-yl)-3-(4-methoxy-3-((3-methylbut-2-en-1-yl)oxy)phenyl)prop-2-en-1-one (10a). Yield: 60%; light yellow liquid; ¹H NMR (CDCl₃, 400 MHz) δ : 1.50 (s, 3H), 1.61 (s, 3H), 1.72–1.77 (m, 6H), 3.87 (s, 3H), 3.89 (s, 3H), 4.59 (d, 2H, *J* = 6.4 Hz), 5.53 (m, 1H), 5.62 (d, 1H, *J* = 10.0 Hz), 6.50 (d, 1H, *J* = 8.8 Hz), 6.68 (d, 1H, *J* = 9.6 Hz), 6.85–6.88 (m, 1H), 7.14–7.17 (m, 2H), 7.56 (d, 1H, *J* = 16.0 Hz), 7.62 (d, 1H, *J* = 16.0 Hz), 7.70 (d, 1H, *J* = 8.8 Hz); ¹³C NMR (CDCl₃, 100 MHz) δ : 18.1, 25.9, 28.0, 28.0, 55.8, 56.0, 65.6, 76.8, 103.5, 108.6, 112.4, 116.9, 119.5, 121.9, 122.2, 126.2, 127.4, 128.7, 128.8, 131.6, 138.1, 140.1, 140.3, 148.4, 151.3, 158.3, 189.9. MS found (M + H)⁺ (*m/z*): 435.27. HPLC purity = 98.9%.

4.1.1.2. (E)-1-(5-Methoxy-2,2-dimethyl-2H-chromen-8-yl)-3-(4-methoxy-3-(prop-2-yn-1-yloxy)phenyl)prop-2-en-1-one (10b). Yield: 47%; light yellow liquid; ¹H NMR (CDCl₃, 400 MHz) δ : 1.52 (s, 6H), 2.52 (s, 1H), 3.89 (s, 3H), 3.92 (s, 3H), 4.80 (s, 2H), 5.63 (d, 1H, *J* = 10.0 Hz), 6.51 (d, 1H, *J* = 8.4 Hz), 6.69 (d, 1H, *J* = 10.0 Hz), 6.91 (d, 1H, *J* = 8.0 Hz), 7.23–7.31 (m, 2H), 7.58 (d, 1H, *J* = 15.6 Hz), 7.65 (d, 1H, *J* = 15.6 Hz), 7.71 (d, 1H, *J* = 8.8 Hz); ¹³C NMR (DMSO, 100 MHz) δ : 27.6, 27.6, 55.6, 55.8, 55.9, 76.8, 78.5, 79.0, 104.1, 109.8, 112.1, 112.3, 115.9, 121.2, 123.7, 124.9, 127.3, 129.3, 131.0, 141.5, 146.6, 151.3, 152.6, 157.7, 188.8. MS found (M + H)⁺ (*m/z*): 405.17. HPLC purity = 98.1%.

4.1.1.3. (E)-3-(3-(Allyloxy)-4-methoxyphenyl)-1-(5-methoxy-2,2-dimethyl-2H-chromen-8-yl)prop-2-en-1-one (10c). Yield: 61%; light yellow liquid; ¹H NMR (CDCl₃, 400 MHz) δ : 1.50 (s, 6H), 3.88 (s, 3H), 3.91 (s, 3H), 4.63 (d, 2H, *J* = 4.0 Hz), 5.28 (dd, 1H, *J* = 9.2 Hz, 1.6 Hz), 5.38 (dd, 1H, *J* = 17.2 Hz, 1.6 Hz), 5.61 (d, 1H, *J* = 10.0 Hz), 6.04–6.12 (m, 1H), 6.50 (d, 1H, *J* = 8.8 Hz), 6.68 (d, 1H, *J* = 10.0 Hz), 6.89 (d, 1H, *J* = 8.4 Hz), 7.14 (d, 1H, *J* = 2.0 Hz), 7.19 (dd, 1H, *J* = 8.4 Hz, 1.6 Hz), 7.54 (d, 1H, *J* = 15.6 Hz), 7.60 (d, 1H, *J* = 15.6 Hz), 7.71 (d, 1H, *J* = 8.4 Hz); ¹³C NMR (DMSO, 100 MHz) δ : 27.5, 27.5, 55.6, 55.9, 68.8, 76.7, 104.1, 109.8, 111.8, 112.0, 116.0, 117.5, 121.2, 122.8, 124.8, 127.5, 129.3, 131.0, 133.5, 141.5, 151.1, 152.5, 157.7, 163.4, 188.8. MS found (M + H)⁺ (*m/z*): *m/z* 407.21. HPLC purity = 97.9%.

4.1.1.4. (E)-3-(3-(2-Hydroxyethoxy)-4-methoxyphenyl)-1-(5-methoxy-2,2-dimethyl-2H-chromen-8-yl)prop-2-en-1-one (10d). Yield: 70%; light yellow solid; ¹H NMR (CDCl₃, 400 MHz) δ : 1.51 (s, 6H), 3.89 (s, 6H), 3.98 (t, 2H, *J* = 4.4 Hz), 4.16 (t, 2H, *J* = 4.4 Hz), 5.62 (d, 1H, *J* = 10.0 Hz), 6.51 (d, 1H, *J* = 8.8 Hz), 6.69 (d, 1H, *J* = 10.0 Hz), 6.90 (d, 1H, *J* = 8.4 Hz), 7.20 (d, 1H, *J* = 1.6 Hz), 7.57 (d, 1H, *J* = 16.0 Hz), 7.62 (d, 1H, *J* = 16.0 Hz); ¹³C NMR (DMSO, 100 MHz) δ : 27.5, 27.5, 55.5, 55.9, 59.5, 70.1, 76.7, 104.1, 109.8, 111.3, 111.9, 116.0, 121.2, 122.6, 124.8, 127.6, 129.3, 131.0, 141.6, 148.3, 151.0, 152.6, 157.7, 188.8. MS found (M + H)⁺ (*m/z*): 411.27. HPLC purity = 98.8%.

4.1.2. General preparation of **10e–h** (method B)

To a solution of compound **9** (0.59 g, 1.6 mmol) in anhydrous DMF (10 mL) under nitrogen was added NaH (0.38 g of a 60% dispersion,

9.5 mmol, 6 equiv). The mixture was stirred at room temperature over 30 min, by which point H₂ evolution had ceased. The reaction mixture was heated to 90 °C, and the halogenated compound (3.6 mmol, 2.25 equiv) was added in portions over 30 min. The reaction mixture was stirred at 90 °C for another 12 h. The completion of the reaction was monitored by TLC. On completion, the mixture was cooled to ambient temperature, and isopropyl alcohol (3 mL) was added to destroy excess NaH. The slurry was partitioned between water (50 mL) and ethyl acetate (50 mL), and the water was extracted with ethyl acetate (3 × 20 mL). The combined ethereal extract was dried (Na₂SO₄), filtered, and concentrated in vacuo to yield a brown oil. Chromatographic separation (hexanes–ethyl acetate–triethylamine, 10:5:1) gave the product as a pale yellow oil.

4.1.2.1. (E)-1-(5-Methoxy-2,2-dimethyl-2H-chromen-8-yl)-3-(4-methoxy-3-(2-morpholinoethoxy)phenyl)prop-2-en-1-one (10e). Yield: 23%; yellow liquid; ¹H NMR (CDCl₃, 400 MHz) δ: 1.50 (s, 6H), 2.63 (t, 4H, J = 4.8 Hz), 2.90 (t, 2H, J = 5.6 Hz), 3.75 (t, 4H, J = 4.8 Hz), 3.90 (s, 6H), 4.19 (t, 2H, J = 5.6 Hz), 5.62 (d, 1H, J = 10.0 Hz), 6.51 (d, 1H, J = 8.8 Hz), 6.69 (d, 1H, J = 10.0 Hz), 6.88 (d, 1H, J = 8.4 Hz), 7.16 (d, 1H, J = 2.0 Hz), 7.19 (dd, 1H, J = 8.4 Hz, 2.0 Hz), 7.52 (d, 1H, J = 15.6 Hz), 7.60 (d, 1H, J = 16.0 Hz), 7.69 (d, 1H, J = 9.2 Hz); ¹³C NMR (DMSO, 100 MHz) δ: 28.0, 28.0, 54.1, 55.8, 56.0, 56.1, 57.3, 57.4, 66.8, 66.9, 76.7, 103.6, 110.7, 111.3, 112.0, 116.8, 121.8, 122.6, 125.5, 127.6, 128.5, 130.1, 141.5, 148.4, 151.1, 153.5, 158.4, 190.8. MS found (M + H)⁺ (m/z): 480.31. HPLC purity = 96.8%.

4.1.2.2. (E)-1-(5-Methoxy-2,2-dimethyl-2H-chromen-8-yl)-3-(4-methoxy-3-(2-(pyrrolidin-1-yl)ethoxy)phenyl)prop-2-en-1-one (10f). Yield: 65%; yellow liquid; ¹H NMR (CDCl₃, 400 MHz) δ: 1.51 (s, 6H), 1.81–1.82 (m, 4H), 2.65–2.66 (m, 4H), 2.98 (t, 2H, J = 6.4 Hz), 3.84 (s, 6H), 4.20 (t, 2H, J = 6.4 Hz), 5.62 (d, 1H, J = 10.0 Hz), 6.51 (d, 1H, J = 8.8 Hz), 6.69 (d, 1H, J = 10.0 Hz), 6.90 (d, 1H, J = 8.4 Hz), 7.20 (d, 1H, J = 1.6 Hz), 7.21 (dd, J = 8.8 Hz, 1.6 Hz), 7.57 (d, 1H, J = 16.0 Hz), 7.62 (d, 1H, J = 16.0 Hz), 7.70 (d, 1H, J = 8.4 Hz); ¹³C NMR (CDCl₃, 100 MHz) δ: 23.5, 23.5, 28.0, 28.0, 54.5, 54.5, 54.8, 55.7, 55.9, 67.7, 76.7, 103.5, 110.4, 111.5, 111.8, 116.8, 121.9, 122.8, 125.4, 128.5, 128.6, 131.6, 141.5, 148.4, 151.3, 153.5, 158.3, 189.8. MS found (M + H)⁺ (m/z): 464.31. HPLC purity = 97.8%.

4.1.2.3. (E)-1-(5-Methoxy-2,2-dimethyl-2H-chromen-8-yl)-3-(4-methoxy-3-(2-(piperidin-1-yl)ethoxy)phenyl)prop-2-en-1-one (10g). Yield: 53%; yellow liquid; ¹H NMR (CDCl₃, 400 MHz) δ: 1.24–1.28 (m, 2H), 1.51 (s, 6H), 1.62–1.64 (m, 4H), 2.56–2.57 (m, 4H), 2.89 (t, 2H, J = 6.4 Hz), 3.84 (s, 6H), 4.20 (t, 2H, J = 6.4 Hz), 5.62 (d, 1H, J = 10.0 Hz), 6.51 (d, 1H, J = 8.8 Hz), 6.69 (d, 1H, J = 10.0 Hz), 6.88 (d, 1H, J = 8.0 Hz), 7.17–7.20 (m, 2H), 7.56 (d, 1H, J = 15.6 Hz), 7.62 (d, 1H, J = 15.6 Hz), 7.70 (d, 1H, J = 8.8 Hz); ¹³C NMR (CDCl₃, 100 MHz) δ: 23.1, 24.7, 24.7, 27.0, 27.0, 53.9, 54.8, 54.9, 56.6, 64.8, 67.7, 76.7, 102.4, 109.4, 110.5, 110.8, 116.0, 120.7, 122.0, 124.4, 128.5, 128.6, 130.6, 141.5, 147.4, 151.3, 153.5, 157.4, 189.0. MS found (M + H)⁺ (m/z): 478.36. HPLC purity = 97.3%.

4.1.2.4. (E)-3-(3-(3-(Dimethylamino)propoxy)-4-methoxyphenyl)-1-(5-methoxy-2,2-dimethyl-2H-chromen-8-yl)prop-2-en-1-one (10h). Yield: 59%; yellow liquid; ¹H NMR (CDCl₃, 400 MHz) δ: 1.50 (s, 6H), 2.04–2.07 (m, 2H), 2.28 (s, 6H), 2.50 (t, 2H, J = 6.4 Hz), 3.85 (s, 6H), 4.09 (t, 2H, J = 6.4 Hz), 5.61 (d, 1H, J = 10.0 Hz), 6.50 (d, 1H, J = 9.2 Hz), 6.68 (d, 1H, J = 10.0 Hz), 6.86 (d, 1H, J = 8.0 Hz), 7.15–7.17 (m, 2H), 7.56 (d, 1H, J = 16.0 Hz), 7.61 (d, 1H, J = 16.0 Hz), 7.69 (d, 1H, J = 8.8 Hz); ¹³C NMR (DMSO, 100 MHz) δ: 26.6, 27.5, 27.5, 44.9, 44.9, 55.4, 55.6, 55.9, 66.5, 76.7, 104.1, 109.8, 111.0, 111.9, 116.0, 121.2, 122.8, 124.8, 127.6, 129.2, 131.1, 141.4, 148.3, 151.1, 152.6, 157.8, 188.6. MS found (M + H)⁺ (m/z): 452.30. HPLC purity = 97.6%.

4.1.3. General preparation of 10i–k (method C)

To the solution of Compound **9** (184 mg, 0.5 mmol) in 5 mL of pyridine was added the requisite anhydride (1 mL). The reaction mixture was stirred at room temperature for 6 h. After removal of the solvent, the compound was purified by flash chromatography using petroleum ether/ethyl acetate (10:1) as eluent and yielded a pale yellow solid.

4.1.3.1. (E)-2-Methoxy-5-(3-(5-methoxy-2,2-dimethyl-2H-chromen-8-yl)-3-oxoprop-1-en-1-yl)phenyl propionate (10i). Yield: 72%; light yellow solid; ¹H NMR (CDCl₃, 400 MHz) δ: 1.29 (t, 3H, J = 6.4 Hz), 1.49 (s, 6H), 2.64 (q, 2H, J = 7.6 Hz), 3.87 (s, 3H), 3.89 (s, 3H), 5.62 (d, 1H, J = 10.0 Hz), 6.51 (d, 1H, J = 8.4 Hz), 6.68 (d, 1H, J = 10.0 Hz), 6.97 (d, 1H, J = 8.4 Hz), 7.29 (d, 1H, J = 2.0 Hz), 7.43 (dd, 1H, J = 8.4 Hz, 2.0 Hz), 7.55 (d, 1H, J = 15.6 Hz), 7.60 (d, 1H, J = 15.6 Hz), 7.70 (d, 1H, J = 8.4 Hz). ¹³C NMR (CDCl₃, 100 MHz) δ: 9.2, 27.4, 28.0, 28.0, 55.8, 56.0, 76.9, 103.4, 110.4, 112.4, 116.8, 121.7, 122.2, 126.2, 127.4, 128.7, 128.8, 131.6, 140.1, 140.3, 152.7, 153.6, 158.3, 172.3, 189.8. MS found (M + H)⁺ (m/z): 423.18. HPLC purity = 99.6%.

4.1.3.2. (E)-2-Methoxy-5-(3-(5-methoxy-2,2-dimethyl-2H-chromen-8-yl)-3-oxoprop-1-en-1-yl)phenyl pentanoate (10j). Yield: 65%; light yellow solid; ¹H NMR (CDCl₃, 400 MHz) δ: 0.97 (t, 3H, J = 7.2 Hz), 1.43–1.47 (m, 2H), 1.48 (s, 6H), 1.76 (quint, 2H, J = 7.6 Hz), 2.59 (t, 2H, J = 7.2 Hz), 3.86 (s, 3H), 3.88 (s, 3H), 5.61 (d, 1H, J = 10.0 Hz), 6.50 (d, 1H, J = 8.8 Hz), 6.67 (d, 1H, J = 10.0 Hz), 6.96 (d, 1H, J = 8.4 Hz), 7.25 (d, 1H, J = 2.0 Hz), 7.42 (dd, 1H, J = 8.4 Hz, 2.0 Hz), 7.58–7.60 (m, 2H), 7.69 (d, 1H, J = 8.8 Hz). ¹³C NMR (CDCl₃, 100 MHz) δ: 13.8, 22.2, 27.1, 28.0, 28.0, 33.7, 55.8, 56.0, 76.9, 103.5, 110.4, 112.4, 116.8, 121.7, 122.1, 126.2, 127.5, 128.7, 128.8, 131.7, 140.1, 140.4, 152.6, 153.6, 158.4, 171.7, 189.8. MS found (M + H)⁺ (m/z): 451.24. HPLC purity = 99.5%.

4.1.3.3. (E)-2-Methoxy-5-(3-(5-methoxy-2,2-dimethyl-2H-chromen-8-yl)-3-oxoprop-1-en-1-yl)phenyl isobutyrate (10k). Yield: 70%; light yellow solid; ¹H NMR (CDCl₃, 400 MHz) δ: 1.32 (s, 3H), 1.34 (s, 3H), 1.49 (s, 6H), 2.85 (m, 1H, J = 7.6 Hz), 3.86 (s, 3H), 3.88 (s, 3H), 5.62 (d, 1H, J = 10.0 Hz), 6.50 (d, 1H, J = 8.8 Hz), 6.68 (d, 1H, J = 10.0 Hz), 6.96 (d, 1H, J = 8.4 Hz), 7.27–7.29 (m, 1H), 7.41 (d, 1H, J = 8.8 Hz), 7.59–7.61 (m, 2H), 7.70 (d, 1H, J = 8.8 Hz); ¹³C NMR (CDCl₃, 100 MHz) δ: 19.0, 19.0, 28.0, 28.0, 34.0, 55.8, 56.0, 76.9, 103.5, 110.4, 112.3, 116.8, 121.7, 122.0, 126.2, 127.5, 128.7, 128.8, 131.7, 140.2, 140.4, 152.7, 153.6, 158.4, 175.0, 189.7. MS found (M + H)⁺ (m/z): 437.22. HPLC purity = 99.2%.

4.1.4. General preparation of 10l–n (method D)

Compound **9** (147.3 mg, 0.4 mmol) was dissolved in dry CH₂Cl₂ (10 mL). Then, requisite acyl chloride was added (0.6 mmol), followed by triethylamine (0.6 mmol, dropwise), and the reaction mixture was stirred at room temperature for 6 h. Reaction progress was followed by TLC. The reaction mixture was washed with: 5 mL 0.1 M HCl and 2 × 5 mL NaCl brine (pH ~ 6). The organic phase was dried with Na₂SO₄, filtered, the solvent was evaporated and the product was dried under vacuum (a pale yellow solid).

4.1.4.1. (E)-2-Methoxy-5-(3-(5-methoxy-2,2-dimethyl-2H-chromen-8-yl)-3-oxoprop-1-en-1-yl)phenyl acrylate (10l). Yield: 43%; light yellow solid; ¹H NMR (CDCl₃, 400 MHz) δ: 1.49 (s, 6H), 3.88 (s, 6H), 5.62 (d, 1H, J = 10.0 Hz), 6.02 (d, 1H, J = 10.4 Hz), 6.36 (dd, 1H, J = 17.2 Hz, 10.4 Hz), 6.50 (d, 1H, J = 8.4 Hz), 6.62 (d, 1H, J = 17.2 Hz), 6.68 (d, 1H, J = 10.0 Hz), 6.98 (d, 1H, J = 8.8 Hz), 7.32 (d, 1H, J = 2.0 Hz), 7.46 (dd, 1H, J = 8.4 Hz, 2.0 Hz), 7.54 (d, 1H, J = 15.6 Hz), 7.59 (d, 1H, J = 15.6 Hz), 7.70 (d, 1H, J = 8.8 Hz); ¹³C NMR (DMSO, 100 MHz) δ: 27.5, 27.5, 55.9, 56.0, 76.7, 104.1, 109.8, 113.2, 116.0,

121.1, 122.4, 125.8, 127.2, 127.4, 127.9, 129.3, 131.0, 133.9, 139.2, 140.1, 152.5, 152.6, 157.8, 163.4, 188.7. MS found (M + H)⁺ (*m/z*): 421.17. HPLC purity = 99.1%.

4.1.4.2. (*E*)-2-Methoxy-5-(3-(5-methoxy-2,2-dimethyl-2H-chromen-8-yl)-3-oxoprop-1-en-1-yl)phenyl 2-chloroacetate (**10m**). Yield: 73%; light yellow solid; ¹H NMR (CDCl₃, 400 MHz) δ: 1.49 (s, 6H), 3.88 (s, 6H), 4.35 (s, 2H), 5.62 (d, 1H, *J* = 10.0 Hz), 6.50 (d, 1H, *J* = 8.8 Hz), 6.68 (d, 1H, *J* = 10.0 Hz), 6.99 (d, 1H, *J* = 8.4 Hz), 7.33 (d, 1H, *J* = 2.0 Hz), 7.46 (dd, 1H, *J* = 8.4 Hz, 1.6 Hz), 7.54 (d, 1H, *J* = 15.6 Hz), 7.59 (d, 1H, *J* = 15.6 Hz), 7.70 (d, 1H, *J* = 8.8 Hz); ¹³C NMR (DMSO, 100 MHz) δ: 27.5, 27.5, 40.8, 55.9, 56.1, 76.7, 104.1, 109.8, 113.4, 116.0, 121.0, 122.0, 125.9, 127.8, 127.9, 131.0, 139.1, 140.0, 152.2, 152.7, 157.8, 165.7, 188.7. MS found (M + H)⁺ (*m/z*): 443.08. HPLC purity = 98.8%.

4.1.4.3. (*E*)-2-Methoxy-5-(3-(5-methoxy-2,2-dimethyl-2H-chromen-8-yl)-3-oxoprop-1-en-1-yl)phenyl cyclopropanecarboxylate (**10n**). Yield: 67%; light yellow solid; ¹H NMR (CDCl₃, 400 MHz) δ: 1.02–1.06 (m, 2H), 1.17–1.20 (m, 2H), 1.49 (s, 6H), 1.88–1.89 (m, 1H), 3.87 (s, 6H), 5.62 (d, 1H, *J* = 10.0 Hz), 6.50 (d, 1H, *J* = 8.8 Hz), 6.68 (d, 1H, *J* = 10.0 Hz), 6.96 (d, 1H, *J* = 8.4 Hz), 7.31 (d, 1H, *J* = 2.0 Hz), 7.42 (dd, 1H, *J* = 8.4 Hz, 2.0 Hz), 7.54 (d, 1H, *J* = 15.6 Hz), 7.59 (d, 1H, *J* = 15.6 Hz), 7.69 (d, 1H, *J* = 8.8 Hz); ¹³C NMR (CDCl₃, 100 MHz) δ: 9.3, 9.3, 12.8, 28.0, 28.0, 55.8, 56.1, 76.9, 103.4, 110.4, 112.4, 116.8, 121.7, 122.3, 126.2, 127.4, 128.7, 128.8, 131.7, 140.0, 140.4, 152.7, 153.6, 158.3, 172.9, 189.9. MS found (M + H)⁺ (*m/z*): 435.14. HPLC purity = 98.9%.

4.1.5. General preparation of **10o–x** (method E)

Requisite acid (0.45 mmol) was added to a stirred mixture of compound **9** (147.3 mg, 0.4 mmol), EDCl (115.0 mg, 0.6 mmol), DMAP (24.4 mg, 0.2 mmol) in anhydrous CH₂Cl₂ (5 mL). The mixture was stirred at room temperature for 12 h. On completion, the slurry was partitioned between water (20 mL) and CH₂Cl₂ (20 mL), and the water was extracted with CH₂Cl₂ (3 × 10 mL). The combined extract of CH₂Cl₂ and the solvent was removed under reduced pressure to yield a yellow solid. Chromatographic separation (petroleum ether–ethyl acetate, 10:1) gave the product as a pale yellow solid.

4.1.5.1. (*E*)-2-Methoxy-5-(3-(5-methoxy-2,2-dimethyl-2H-chromen-8-yl)-3-oxoprop-1-en-1-yl)phenyl 3-methoxybenzoate (**10o**). Yield: 82%; light yellow solid; ¹H NMR (CDCl₃, 400 MHz) δ: 1.49 (s, 6H), 3.86 (s, 9H), 5.61 (d, 1H, *J* = 10.0 Hz), 6.50 (d, 1H, *J* = 8.8 Hz), 6.67 (d, 1H, *J* = 10.0 Hz), 7.02 (d, 1H, *J* = 8.8 Hz), 7.18 (dd, 1H, *J* = 8.0 Hz, 2.4 Hz), 7.40–7.43 (m, 2H), 7.49 (d, 1H, *J* = 8.4 Hz), 7.57 (d, 1H, *J* = 16.0 Hz), 7.62 (d, 1H, *J* = 16.0 Hz), 7.69–7.72 (m, 2H), 7.82 (d, 1H, *J* = 7.6 Hz); ¹³C NMR (CDCl₃, 100 MHz) δ: 28.0, 28.0, 55.5, 55.8, 56.1, 76.9, 103.5, 110.5, 112.5, 114.6, 116.7, 120.2, 121.7, 122.4, 122.8, 126.3, 127.5, 128.7, 128.9, 129.6, 130.5, 131.6, 140.3, 140.4, 152.8, 153.6, 158.4, 159.7, 164.4, 189.9. MS found (M + H)⁺ (*m/z*): 501.24. HPLC purity = 98.6%.

4.1.5.2. (*E*)-2-Methoxy-5-(3-(5-methoxy-2,2-dimethyl-2H-chromen-8-yl)-3-oxoprop-1-en-1-yl)phenyl 4-bromobenzoate (**10p**). Yield: 64%; light yellow solid; ¹H NMR (CDCl₃, 400 MHz) δ: 1.49 (s, 6H), 3.86 (s, 3H), 3.91 (s, 3H), 5.61 (d, 1H, *J* = 10.0 Hz), 6.51 (d, 1H, *J* = 8.4 Hz), 6.67 (d, 1H, *J* = 10.0 Hz), 7.02 (d, 1H, *J* = 8.4 Hz), 7.41 (m, 1H), 7.49 (d, 1H, *J* = 8.0 Hz), 7.59–7.63 (m, 2H), 7.66 (d, 2H, *J* = 8.4 Hz), 7.70 (d, 1H, *J* = 8.4 Hz), 8.07 (d, 2H, *J* = 8.4 Hz). MS found (M + H)⁺ (*m/z*): 549.05. HPLC purity = 98.9%.

4.1.5.3. (*E*)-2-Methoxy-5-(3-(5-methoxy-2,2-dimethyl-2H-chromen-8-yl)-3-oxoprop-1-en-1-yl)phenyl 2-(3-(trifluoromethyl)phenyl)acetate (**10q**). Yield: 69%; light yellow solid; ¹H NMR (CDCl₃, 400 MHz)

δ: 1.44 (s, 6H), 3.80 (s, 3H), 3.87 (s, 3H), 3.96 (s, 2H), 5.60 (d, 1H, *J* = 10.0 Hz), 6.49 (d, 1H, *J* = 9.2 Hz), 6.67 (d, 1H, *J* = 10.0 Hz), 6.94 (d, 1H, *J* = 8.4 Hz), 7.25–7.27 (m, 2H), 7.42 (d, 1H, *J* = 8.8 Hz), 7.49 (d, 1H, *J* = 8.0 Hz), 7.56–7.60 (m, 3H), 7.68–7.98 (m, 2H); ¹³C NMR (CDCl₃, 100 MHz) δ: 27.9, 27.9, 40.7, 55.8, 55.9, 76.9, 103.5, 110.5, 112.4, 116.8, 121.7, 121.9, 124.2, 126.2, 126.2, 126.4, 127.7, 128.7, 128.9, 129.1, 131.7, 132.9, 134.5, 140.0, 140.1, 152.4, 153.6, 158.4, 168.7, 189.7. MS found (M + H)⁺ (*m/z*): 553.27. HPLC purity = 98.2%.

4.1.5.4. (*E*)-2-Methoxy-5-(3-(5-methoxy-2,2-dimethyl-2H-chromen-8-yl)-3-oxoprop-1-en-1-yl)phenyl 2-(3,4-dichlorophenyl)acetate (**10r**). Yield: 70%; light yellow solid; ¹H NMR (CDCl₃, 400 MHz) δ: 1.45 (s, 6H), 3.83 (s, 3H), 3.86 (s, 2H), 3.88 (s, 3H), 5.62 (d, 1H, *J* = 10.0 Hz), 6.50 (d, 1H, *J* = 8.4 Hz), 6.68 (d, 1H, *J* = 10.0 Hz), 6.96 (d, 1H, *J* = 8.4 Hz), 7.23–7.26 (m, 2H), 7.43 (d, 2H, *J* = 8.0 Hz), 7.54–7.58 (m, 3H), 7.70 (d, 1H, *J* = 8.8 Hz); ¹³C NMR (DMSO, 100 MHz) δ: 27.4, 27.4, 38.6, 56.0, 56.1, 76.7, 104.2, 109.8, 113.3, 116.0, 121.0, 122.0, 125.8, 127.7, 127.9, 129.3, 129.8, 129.9, 130.5, 130.8, 131.1, 131.5, 135.0, 139.4, 140.1, 152.4, 152.6, 157.8, 168.8, 188.7. MS found (M + H)⁺ (*m/z*): 553.06. HPLC purity = 98.4%.

4.1.5.5. (*E*)-2-Methoxy-5-((*E*)-3-(5-methoxy-2,2-dimethyl-2H-chromen-8-yl)-3-oxoprop-1-en-1-yl)phenyl 3-(4-methoxyphenyl)acrylate (**10s**). Yield: 72%; light yellow solid; ¹H NMR (CDCl₃, 400 MHz) δ: 1.49 (s, 6H), 3.86 (s, 9H), 5.61 (d, 1H, *J* = 10.0 Hz), 6.51 (d, 1H, *J* = 8.4 Hz), 6.53 (d, 1H, *J* = 15.6 Hz), 6.67 (d, 1H, *J* = 10.0 Hz), 6.93 (d, 2H, *J* = 8.4 Hz), 7.00 (d, 1H, *J* = 8.0 Hz), 7.38 (m, 1H), 7.46 (d, 1H, *J* = 7.6 Hz), 7.55 (d, 2H, *J* = 7.6 Hz), 7.57 (d, 1H, *J* = 14.8 Hz), 7.62 (d, 1H, *J* = 14.8 Hz), 7.70 (d, 1H, *J* = 7.6 Hz), 7.83 (d, 1H, *J* = 15.6 Hz); ¹³C NMR (CDCl₃, 100 MHz) δ: 28.0, 28.0, 55.4, 55.8, 56.1, 76.9, 103.5, 110.5, 112.5, 114.1, 114.4, 114.4, 116.7, 121.7, 122.4, 126.2, 126.9, 127.4, 128.7, 128.9, 130.1, 130.1, 131.6, 140.2, 140.5, 146.6, 152.8, 153.6, 158.4, 161.8, 165.1, 189.9. MS found (M + H)⁺ (*m/z*): 527.26. HPLC purity = 97.5%.

4.1.5.6. (*E*)-2-Methoxy-5-(3-(5-methoxy-2,2-dimethyl-2H-chromen-8-yl)-3-oxoprop-1-en-1-yl)phenyl 4-(4-(bis(2-chloroethyl)amino)phenyl)butanoate (**10t**). Yield: 39%; light yellow solid; ¹H NMR (CDCl₃, 400 MHz) δ: 1.48 (s, 6H), 2.03–2.07 (m, 2H), 2.61 (t, 2H, *J* = 7.2 Hz), 2.68 (t, 2H, *J* = 7.2 Hz), 3.64 (t, 4H, *J* = 6.8 Hz), 3.72 (t, 4H, *J* = 6.8 Hz), 3.87 (s, 3H), 3.89 (s, 3H), 5.61 (d, 1H, *J* = 10.0 Hz), 6.51 (d, 1H, *J* = 8.8 Hz), 6.66 (d, 2H, *J* = 8.0 Hz), 6.68 (d, 1H, *J* = 10.0 Hz), 6.98 (d, 1H, *J* = 8.4 Hz), 7.12 (d, 2H, *J* = 8.0 Hz), 7.27 (m, 1H), 7.44 (d, 1H, *J* = 8.4 Hz), 7.56 (d, 1H, *J* = 14.8 Hz), 7.59 (d, 1H, *J* = 14.8 Hz), 7.70 (d, 1H, *J* = 8.8 Hz); ¹³C NMR (CDCl₃, 100 MHz) δ: 26.9, 28.0, 28.0, 33.3, 33.8, 40.5, 40.5, 53.6, 53.6, 55.8, 55.9, 76.9, 103.5, 110.4, 110.4, 112.2, 112.4, 116.7, 121.7, 122.2, 126.2, 127.3, 128.7, 128.8, 129.8, 129.8, 130.5, 131.6, 140.0, 144.4, 152.6, 153.6, 158.4, 171.4, 189.8. MS found (M + H)⁺ (*m/z*): 652.33. HPLC purity = 96.8%.

4.1.5.7. (*E*)-2-Methoxy-5-(3-(5-methoxy-2,2-dimethyl-2H-chromen-8-yl)-3-oxoprop-1-en-1-yl)phenyl furan-2-carboxylate (**10u**). Yield: 88%; light yellow solid; ¹H NMR (CDCl₃, 400 MHz) δ: 1.49 (s, 6H), 3.86 (s, 6H), 5.61 (d, 1H, *J* = 10.0 Hz), 6.50 (d, 1H, *J* = 8.4 Hz), 6.60–6.64 (m, 1H), 6.67 (d, 1H, *J* = 10.0 Hz), 7.01 (d, 2H, *J* = 8.4 Hz), 7.41 (m, 2H), 7.48 (d, 1H, *J* = 8.4 Hz), 7.56 (d, 1H, *J* = 15.6 Hz), 7.61 (d, 1H, *J* = 15.6 Hz), 7.68 (m, 1H), 7.70 (d, 1H, *J* = 8.8 Hz); ¹³C NMR (DMSO, 100 MHz) δ: 27.5, 27.5, 55.9, 56.1, 76.7, 104.1, 109.8, 112.8, 113.3, 115.9, 120.4, 121.1, 122.7, 125.9, 127.5, 127.9, 129.3, 131.0, 138.7, 140.1, 142.6, 148.7, 152.5, 152.6, 155.7, 157.8, 188.9. MS found (M + H)⁺ (*m/z*): 461.13. HPLC purity = 98.6%.

4.1.5.8. (*E*)-2-Methoxy-5-(3-(5-methoxy-2,2-dimethyl-2H-chromen-8-yl)-3-oxoprop-1-en-1-yl)phenyl methanesulfonate (**10v**). Yield: 78%;

light yellow solid; ^1H NMR (CDCl_3 , 400 MHz) δ : 1.52 (s, 6H), 3.89 (s, 3H), 3.94 (s, 3H), 5.63 (d, 1H, $J = 10.0$ Hz), 6.52 (d, 1H, $J = 8.8$ Hz), 6.68 (d, 1H, $J = 10.0$ Hz), 7.01 (d, 2H, $J = 8.8$ Hz), 7.46 (dd, 1H, $J = 8.4$ Hz, 2.0 Hz), 7.59 (d, 1H, $J = 15.6$ Hz), 7.61 (d, 1H, $J = 2.0$ Hz), 7.65 (d, 1H, $J = 15.6$ Hz), 7.72 (d, 1H, $J = 8.8$ Hz); ^{13}C NMR (CDCl_3 , 100 MHz) δ : 28.0, 28.0, 38.3, 55.8, 56.2, 77.1, 103.5, 110.5, 112.9, 116.6, 121.4, 123.0, 126.9, 128.8, 129.2, 129.3, 131.7, 138.5, 139.4, 152.6, 153.8, 158.5, 189.4. MS found $(\text{M} + \text{H})^+$ (m/z): 445.10. HPLC purity = 98.2%.

4.1.5.9. (*E*)-2-Methoxy-5-(3-(5-methoxy-2,2-dimethyl-2H-chromen-8-yl)-3-oxoprop-1-en-1-yl)phenyl phenylmethanesulfonate (**10w**). Yield: 81%; light yellow solid; ^1H NMR (CDCl_3 , 400 MHz) δ : 1.51 (s, 6H), 3.88 (s, 3H), 3.93 (s, 3H), 4.59 (s, 2H), 5.61 (d, 1H, $J = 10.0$ Hz), 6.51 (d, 1H, $J = 8.8$ Hz), 6.67 (d, 1H, $J = 10.0$ Hz), 6.99 (d, 1H, $J = 8.4$ Hz), 7.26–7.29 (m, 1H), 7.36–7.49 (m, 6H), 7.52 (d, 1H, $J = 15.6$ Hz), 7.57 (d, 1H, $J = 15.6$ Hz), 7.70 (d, 1H, $J = 8.8$ Hz); ^{13}C NMR (CDCl_3 , 100 MHz) δ : 28.0, 28.0, 55.8, 56.2, 57.6, 77.2, 103.5, 110.5, 112.8, 116.6, 121.5, 122.9, 126.9, 127.4, 128.8, 128.8, 128.9, 128.9, 129.2, 129.2, 130.9, 130.9, 131.7, 138.7, 139.5, 152.8, 153.8, 158.5, 189.6. MS found $(\text{M} + \text{H})^+$ (m/z): 521.14. HPLC purity = 98.0%.

4.1.5.10. (*E*)-2-Methoxy-5-(3-(5-methoxy-2,2-dimethyl-2H-chromen-8-yl)-3-oxoprop-1-en-1-yl)phenyl 4-methylbenzenesulfonate (**10x**). Yield: 79%; light yellow solid; ^1H NMR (CDCl_3 , 400 MHz) δ : 1.52 (s, 6H), 2.35 (s, 3H), 3.60 (s, 3H), 3.89 (s, 3H), 5.63 (d, 1H, $J = 10.0$ Hz), 6.51 (d, 1H, $J = 8.8$ Hz), 6.68 (d, 1H, $J = 10.0$ Hz), 6.83 (d, 1H, $J = 8.4$ Hz), 7.29 (d, 1H, $J = 8.0$ Hz), 7.38 (dd, 1H, $J = 8.8$ Hz, 2.0 Hz), 7.44 (d, 1H, $J = 2.0$ Hz), 7.53 (d, 1H, $J = 16.0$ Hz), 7.58 (d, 1H, $J = 15.6$ Hz), 7.71 (d, 1H, $J = 8.8$ Hz), 7.74 (d, 1H, $J = 8.4$ Hz); ^{13}C NMR (CDCl_3 , 100 MHz) δ : 21.7, 28.0, 28.0, 55.8, 55.9, 77.2, 103.5, 110.5, 112.7, 116.5, 121.5, 122.9, 126.9, 128.6, 128.6, 128.7, 128.8, 128.8, 129.2, 129.2, 131.7, 132.9, 138.7, 139.5, 145.2, 153.1, 153.8, 158.5, 189.6. MS found $(\text{M} + \text{H})^+$ (m/z): 521.19. HPLC purity = 98.2%.

4.2. Biological assay methods

4.2.1. Tissue culture and reagents

Taxol was purchased from Sigma. Cell lines were purchased from American Type Culture Collection (ATCC) and maintained following ATCC recommendations. Cell lines were routinely grown in DMEM or RPM1 (CellGro) supplemented with 10% fetal bovine serum (Cell-Generation, CO) and 1 unit/mL penicillin–streptomycin (Gibco).

4.2.2. Cell proliferation assay

Antiproliferative activities were maintained in the HepG2 cells, A375 cells, K562 cells, normal cell line L02 cells. Cells in logarithmic phase were diluted to a density of 40,000–50,000 cells/mL in culture medium based on growth characteristics, supplemented with 10% fetal bovine serum, 2 mM glutamine and antibiotics, at 37 °C in humid atmosphere of 5% CO_2 . Cells were seeded on 96-well plates and selected compound were added at various doses for indicated durations. MTT was then added for 4-h incubation. The MTT formazan precipitate was then dissolved in DMSO, and the absorbance was measured at a wave length of 590 nm.

4.2.3. Flow cytometry

HepG2 cells were incubated with various concentrations (0.2, 1 μM) of selected compound or DMSO vehicle for 24 h at 37 °C in an incubator supplemented with 5% CO_2 . Then cells were fixed in ice-cold 70% ethanol overnight at 4 °C. The cell DNA was stained with 5 $\mu\text{g/mL}$ propidium iodide containing 10 $\mu\text{g/mL}$ of DNase-free RNase at 4 °C for a minimum of 10 min. After treatment, the cells were collected and the DNA content was analyzed by flow cytometer (TASC240, USA).

4.2.4. Tubulin staining

HepG2 cells were grown on glass covers lip sin 6-well plates and treated with 1 μM selected compound for 24 h. Then cells were washed with 1 \times PBS once, fixed in cold 4% PFA for 10 min. After 1 h blocking with 5% goat serum albumin/0.3% Triton/PBS, the cells were incubated with monoclonal anti- α tubulin (Santa Cruz) overnight at 4 °C, washed in PBS and incubated with Alexa Fluor 488 goat anti-mouse IgG (H + L; Invitrogen) for 30 min at room temperature. Cells were washed in PBS and microtubule distribution imaged on either an Olympus IX81 fluorescence microscope or Bio-Rad MRC1024 confocal microscope. Propidium iodide was added at 5 $\mu\text{g/mL}$ to stain for nuclei.

4.2.5. In vitro tubulin polymerization assay

2 mg/mL Tubulin from pig brain (Cytoskeleton) was resuspended in PEM buffer [80 mM PIPES, (pH 6.9), 0.5 mM EGTA, 2 mM MgCl_2 and 15% glycerol], and then was pre-incubated with compounds or its vehicle DMSO on ice. PEG containing GTP was added to the final concentration of 1 mM before detecting the tubulin polymerization reaction. The reaction was monitored by a spectrophotometer in absorbance at 340 nm at 37 °C every 30 s. The final concentrations of the compound were list as follow: **10i** (5, 10, 20 μM), Taxol (5, 20 μM).

4.2.6. Western blot analysis

Cells were treated with indicated concentrations of the selected test agents for treatment duration. After 24 h treatment, cells were washed with PBS three times. Then added lysis buffer (20 mM Tris–HCl, pH 6.8, 1 mM MgCl_2 , 2 mM EGTA, 1 mM PMSF, 1 mM orthovanadate, 0.5% NP-40 and 20 mg/mL proteinase inhibitor) on ice for 30 min. Supernatants were collected after centrifugation at 15,000 g for 10 min at 4 °C. This yielded soluble tubulin dimers in the supernatant and polymerized microtubules in the pellet. Equal amounts of the two fractions were analyzed by western blot probed with α -tubulin antibody and secondary HRP-conjugated antibody. The blots were developed using an Enhanced Chemiluminescence reagent kit, followed by development on Kodak Bio-MAX MR film (Rochester, NY).

4.2.7. In vivo tumor models

Thirty mice were randomly assigned to five groups. For HepG2 xenografts (5×10^6 per mouse), we used 5–6-week-old female Balb/C and athymic nude mice respectively, implanted the indicated number of cells suspended in 100 μL HBSS in the right flank of mice. Length and width of tumors were measured, and the tumor volume (mm^3) was calculated by the formula, $\pi/6 \times \text{length} \times \text{width}^2$, after tumor cells inoculated 10 days. Six mice per group were randomly assigned. When tumor volumes reached 100 mm^3 , the animals were treated for three weeks at the doses of **10i** (2.5 mg/kg), **10i** (5 mg/kg) and **10i** (10 mg/kg) every two days. And the positive control was Taxol (5 mg/kg) every four days. Signs of toxicity and mortality were observed daily. Tumor volumes and body weights were measured every two days when administered with a caliper (calculated volume (mm^3) = $\pi/6 \times \text{length} \times \text{width} \times \text{width}$). The anti-tumor activity of compound was evaluated by two parameters: T/C value (%) = (tumor volume of treated group)/(Δ tumor volume of control group) \times 100%, and tumor inhibitor = (1 – tumor weight of treat group/tumor weight of control group) \times 100%.

Acknowledgments

The authors greatly appreciate the financial support from National Key Programs of China during the 12th Five-Year Plan Period (2012ZX09103101-009).

Appendix A. Supplementary material

Supplementary material related to this article can be found at <http://dx.doi.org/10.1016/j.ejmech.2013.01.007>.

References

- [1] M.A. Jordan, L. Wilson, *Nat. Rev. Cancer* 4 (2004) 253–265.
- [2] R. Heald, E. Nogales, *J. Cell. Sci.* 115 (2002) 3–4.
- [3] M. Carr, L.M. Greene, A.J. Knox, D.G. Lloyd, D.M. Zisterer, M.J. Meegan, *Eur. J. Med. Chem.* 45 (2010) 5752–5766.
- [4] J.A. Hadfield, S. Ducki, N. Hirst, A.T. McGown, *Prog. Cell. Cycle Res.* 5 (2003) 309–325.
- [5] A. Kruczynski, B.T. Hill, *Crit. Rev. Oncol. Hematol.* 40 (2001) 159–173.
- [6] M.C. Bibby, *Drugs Future* 27 (2002) 475–480.
- [7] A.T. McGown, B.W. Fox, *Cancer Chemother. Pharmacol.* 26 (1990) 79–81.
- [8] P.B. Schiff, J. Fant, S.B. Horwitz, *Nature* 277 (1979) 665–667.
- [9] E.K. Rowinsky, R.C. Donehower, *N. Engl. J. Med.* 332 (1995) 1004–1014.
- [10] E.K. Rowinsky, *Semin. Oncol.* 24 (1997) 1–12.
- [11] G.A. Orr, P. Verdier-Pinard, H. McDaid, S.B. Horwitz, *Oncogene* 22 (2003) 7280–7295.
- [12] D.M. Bollag, P.A. McQueney, J. Zhu, O. Hensens, L. Koupal, J. Liesch, M. Goetz, E. Lazarides, C.M. Woods, *Cancer Res.* 55 (1995) 2325–2333.
- [13] E. Ter Haar, R.J. Kowalski, E. Hamel, C.M. Lin, R.E. Longely, S.P. Gunasekara, H.S. Rosenkranz, D.W. Day, *Biochemistry* 35 (1996) 243–250.
- [14] J.H. Stephen, U.M. Thomas, T.M. David, F. Rejza, W.K. Randall, J.M. Timothy, L.S. Stuart, *Chem. Biol.* 7 (2000) 275–286.
- [15] S. Yasushi, T. Toshimasa, N. Yukimasa, *Cancer Chemother. Pharmacol.* 40 (1997) 513–520.
- [16] M.V. Reddy, B. Akula, S.C. Cosenza, C.M. Lee, M.R. Mallireddigari, V.R. Pallela, D.R. Subbaiah, A. Udofa, E.P. Reddy, *J. Med. Chem.* 55 (2012) 5174–5187.
- [17] H.Y. Ye, A. Fu, W.S. Wu, Y.F. Li, G.C. Wang, M.H. Tang, S.C. Li, S.C. He, S.J. Zhong, H.J. Lai, J.H. Yang, M.L. Xiang, A.H. Peng, L.J. Chen, *Fitoterapia* 83 (8) (2012) 1402–1408.
- [18] W.S. Wu, H.Y. Ye, G.C. Wang, X.L. Han, J. Hu, M.H. Tang, X.M. Duan, Y. Fan, S.C. He, L. Huang, H.Y. Pei, X.W. Wang, X.X. Li, C.F. Xie, R.H. Zhang, Z. Yuan, Y.Q. Mao, L.J. Chen, Y.Q. Wei, *Carcinogenesis*, Accepted.
- [19] D.Y. Kim, K.H. Kim, N.D. Kim, K.Y. Lee, C.K. Han, J.H. Yoon, S.K. Moon, S.S. Lee, B.L. Seong, *J. Med. Chem.* 49 (2006) 5664–5670.
- [20] S. Ducki, D. Rennison, M. Woo, A. Kendall, J.F.D. Chabert, A.T. McGown, N.J. Lawrence, *Bioorg. Med. Chem.* 17 (2009) 7698–7710.
- [21] K.C. Nicolaou, J.A. Pfefferkorn, G.Q. Cao, *Angew. Chem. Int. Ed.* 39 (2000) 734–739.
- [22] K.C. Nicolaou, J.A. Pfefferkorn, A.J. Roecker, G.Q. Cao, S. Barleenga, H.J. Mitchell, *J. Am. Chem. Soc.* 122 (2000) 9939–9953.
- [23] T. Narender, S.A. Gupta, *Bioorg. Med. Chem. Lett.* 14 (2004) 3913–3916.
- [24] F. Peng, G.C. Wang, X.X. Li, D. Cao, Z. Yang, L. Ma, H.Y. Ye, X.L. Liang, Y. Ran, J.Y. Chen, J.X. Qiu, C.F. Xie, C.Y. Deng, M.L. Xiang, A.H. Peng, Y.Q. Wei, L.J. Chen, *Eur. J. Med. Chem.* 54 (2012) 272–280.
- [25] G.C. Wang, W.S. Wu, F. Peng, D. Cao, Z. Yang, L. Ma, N. Qiu, H.Y. Ye, X.L. Han, J.Y. Chen, J.X. Qiu, Y. Sang, X.L. Liang, Y. Ran, A.H. Peng, Y.Q. Wei, *Eur. J. Med. Chem.* 54 (2012) 793–803.
- [26] Y.R. Lee, X. Wang, L.K. Xia, *Molecules* 12 (2007) 1420–1429.
- [27] S.K. Kumar, E. Hager, C. Pettit, H. Gurulingappa, N.E. Davidson, S.R. Khan, *J. Med. Chem.* 46 (2003) 2813–2815.
- [28] B.C. Baguley, *Mol. Biotechnol.* 46 (2010) 308–316.
- [29] N.J. Lawrence, A.T. McGown, S. Ducki, J.A. Hadfield, *Anti-Cancer Drug Des.* 15 (2000) 135–141.
- [30] E. Hamel, *Cell. Biochem. Biophys.* 38 (2003) 1–21.